

Analysis of Wireless Power Transfer System Employing Active Shielding with Virtual Inductance and Two-port Equivalent Circuit

Keita Furukawa, Keisuke Kusaka, and Jun-ichi Itoh
Department of Electrical, Electronics and Information Engineering,
Nagaoka University of Technology, NUT
Nagaoka, Niigata, Japan

archer_FK@stn.nagaokaut.ac.jp, kusaka@vos.nagaokaut.ac.jp, itoh@vos.nagaokaut.ac.jp

Abstract—This paper proposes and analyzes an active-shielding method to reduce EMF of wireless power transfer (WPT) systems. Additional power supplies and two windings cancel magnetic field generated by the WPT coils with only reactive power. The advantage of the proposed method is that the capacity of the additional power supplies are small. The parameter variation of the WPT coils and the magnetic field are calculated with a two-port equivalent circuit which the additional power supplies are replaced to virtual inductance in. As a result, the magnetic field decreases by 27.2dB with the proposed method. In addition, the transmitting power is increased as the magnetic field becomes smaller because the equivalent mutual inductance is reduced.

Keywords—active shielding, equivalent circuit, leakage magnetic field, wireless power transfer

I. INTRODUCTION

Electric vehicles (EVs), which do not emit CO₂ during running, are becoming increasingly popular [1]. Battery chargers with cables are mainly used to charge batteries in EVs when EVs are parked in parking places [1]. However, the battery charging process is a burden to users [1]. In addition, electric shock is one of serious risks when the users touch metallic contacts [1].

Wireless power transfer (WPT) systems have been attracted as battery charging systems of EVs to solve the issues [1–4]. The WPT coils generate large radiation noise during the charging operation of the WPT [1]. Electric devices or human bodies near the WPT system are harmed by the radiation noise [1]. Thus, the permissible level of the radiation noise is regulated by various regulations, e.g. the International Commission on Non-Ionizing Radiation Protection 2010 guidelines and International Special Committee on Radio Interference guidelines [5–8].

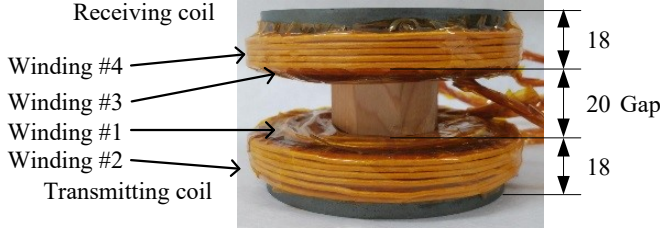
Many methods conducted on modulations, topologies of converters, and configurations of the WPT coils have been suggested to reduce the magnetic field [9–19]. Metallic plates or rings are used to cancel the magnetic field with eddy current in general [12, 14]. However, a reduction in the magnetic field is small, and the temperature of the metallic plates or rings is risen due to eddy current loss. Resonant shielding has been proposed as a method to further reduce the magnetic field [13, 15]. The

resonant shielding uses capacitors and additional windings. The capacitors are connected to the additional windings around the WPT coils. The RMS current flowing on the additional windings is increased with resonance between inductance of the additional windings and capacitance of the capacitors [13, 15]. However, the effective frequency band is limited by design of the resonant frequency [13].

Active shielding has been proposed to solve the issues with the metallic plates or rings, and resonant shielding [14–20]. The active shielding uses additional windings (canceling windings) and power supplies. The canceling windings wound around the WPT coils, are connected to the additional power supplies or the main windings [14–20]. The additional power supplies control the current of the canceling windings to reduce the magnetic field with effect [14–20]. Thus, the advantage of the active shielding is not only that radiation noise is decreased significantly but also that the magnetic field is adjustable depending on the load [14, 15, 18, 19].

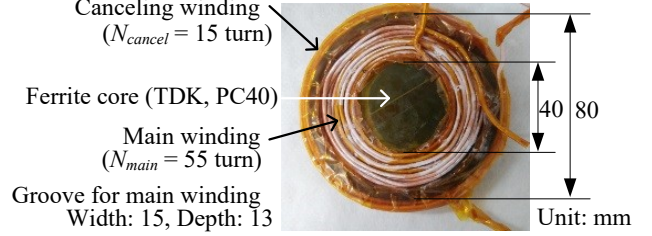
The design method of the active shielding using injected reactance-compensation current has been suggested [20]. Moreover, electrical and magnetic characteristics are clarified with the design method [20]. The current flowing on the canceling windings and the output voltage of the additional power supplies are calculated with the operational current when the canceling windings are short [20]. The features of the design method are that the loss and capacity of the additional power supplies are small, and that how to adjust the magnetic field is demonstrated [20]. However, the operational condition at minimum leakage magnetic field and transmitting power does not agreed with the designed values, because influence of the change in the current of the canceling windings is not considered.

This paper proposes an active shielding method based on the resonant shielding. In addition, the electrical and magnetic characteristics are shown with a two-port equivalent circuit of the WPT coils. The additional power supplies output only reactive power to cancel the magnetic field. The advantage of the proposed method is that the small-capacity additional power supplies are available because the canceling windings do not donate the power transmission. Moreover, suitable operating condition at zero leakage magnetic field at a measurement point



(a) Side view of WPT coils.

Fig. 1. Prototype of WPT coils.



(b) Top view of transmitting coil.

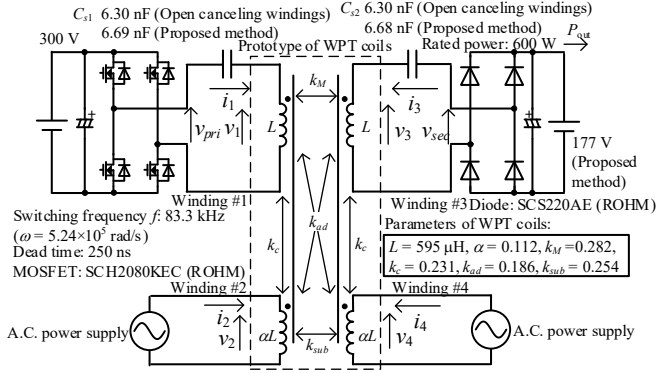


Fig. 2. Experient circuit and conditions.

is calculated. The originality of the proposed method is that a four-winding WPT coils and the operation of the proposed method are converted to the two-port equivalent circuit to simplify analysis.

II. CONFIGURATION OF WPT SYSTEM WITH ACTIVE SHIELDING METHOD

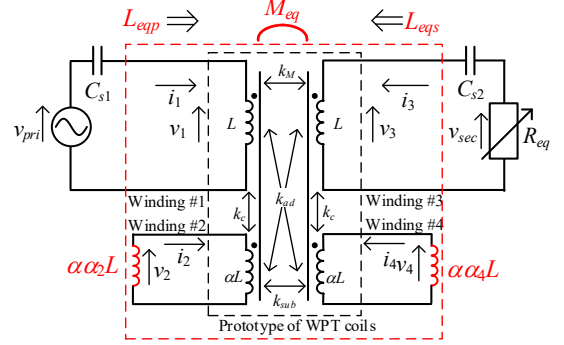
A. Configuration of WPT Circuit

Figure 1 shows the prototype of the four-winding WPT coils. The configuration of the transmitting and receiving coils are identical. The main windings (windings #1 and #3) are wound in the grooves on the cores. The canceling windings (windings #2 and #4) are wound on the side of the cores.

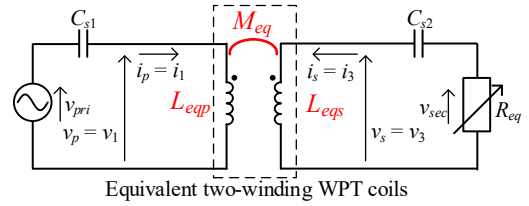
Figure 2 shows the circuit diagram and the conditions of the experiment. The input DC voltage is 300 V. The resonant capacitors are connected to the main windings in series for power factor compensation. The load is the 177-V DC power supply because of the battery load. The parameters of the WPT coils in Fig. 1 (the self-inductance of each winding and the coupling coefficients between each windings) are also shown in Fig. 2. Note that the parameters of the circuit in Fig. 2 are designed to achieve 600-W transmitting power and the resonant condition when the canceling windings are short.

B. Equivalent Circuit of WPT Coils and Equivalent Inductance

Figure 3 shows the equivalent circuit of the WPT coils and the two-port equivalent circuit. The additional power supplies are replaced to the virtual inductance in the equivalent circuit.



(a) Equivalent circuit using virtual inductance.



(b) Equivalent two-port circuit of WPT coils.

Fig. 3. Equivalent circuit of WPT circuit.

The virtual inductance represents the operation of the additional power supplies as passive elements from the terminal voltage and output current. The virtual inductance provides the canceling windings with the reactive power to reduce the leakage magnetic field. The coefficients α_2 and α_4 of the virtual inductance are defined as

$$\begin{cases} \alpha_2 = -\frac{\dot{V}_2}{j\omega\alpha LI_2} & (\omega = 2\pi f_{sw}) \\ \alpha_2 = 0 & (\omega \neq 2\pi f_{sw}) \end{cases} \quad (1),$$

and

$$\begin{cases} \alpha_4 = -\frac{\dot{V}_4}{j\omega\alpha LI_4} & (\omega = 2\pi f_{sw}) \\ \alpha_4 = 0 & (\omega \neq 2\pi f_{sw}) \end{cases} \quad (2),$$

where f_{sw} is the switching frequency of the inverter in Fig. 2, αL is the self-inductance of the canceling windings, I_m is current of winding # m ($m = 1, 2, 3, 4$), and \dot{V}_m is induced voltage of winding # m . The range of α_2 and α_4 is a real number. The coefficients α_2 and α_4 are infinity when the canceling windings are open. Whereas, α_2 and α_4 are zero when the canceling winding are short.

Representing operation of the additional power supplies as the virtual inductance offers several benefits:

- The operation of the additional power supplies is limited not to donate the power transmission.
- The replacement helps conversion of the four-winding WPT coils and the additional power supplies to the two-port network.
- Required apparent power of the additional power supplies is normalized.
- Frequency dependance of the additional power supplies is avoided on later analyses.

The relationship between the current and voltage of the windings is shown in (3) with the inductance matrix \mathbf{L} .

$$\begin{bmatrix} \dot{V}_1 \\ 0 \\ \dot{V}_3 \\ 0 \end{bmatrix} = j\omega \mathbf{L} \begin{bmatrix} \dot{I}_1 \\ \dot{I}_2 \\ \dot{I}_3 \\ \dot{I}_4 \end{bmatrix} \quad (3)$$

$$= j\omega L \begin{bmatrix} 1 & \sqrt{\alpha}k_c & k_M & \sqrt{\alpha}k_{ad} \\ \sqrt{\alpha}k_c & \alpha(1+\alpha_2) & \sqrt{\alpha}k_{ad} & \alpha k_{sub} \\ k_M & \sqrt{\alpha}k_{ad} & 1 & \sqrt{\alpha}k_c \\ \sqrt{\alpha}k_{ad} & \alpha k_{sub} & \sqrt{\alpha}k_c & \alpha(1+\alpha_4) \end{bmatrix} \begin{bmatrix} \dot{I}_1 \\ \dot{I}_2 \\ \dot{I}_3 \\ \dot{I}_4 \end{bmatrix}$$

Here, k_c , k_M , k_{ad} and k_{sub} are the coupling coefficient between two windings. Equation (3) shows that the equivalent circuit in Fig. 3(a) is also the two-port network such as Fig. 3(b) because degree of freedom is two.

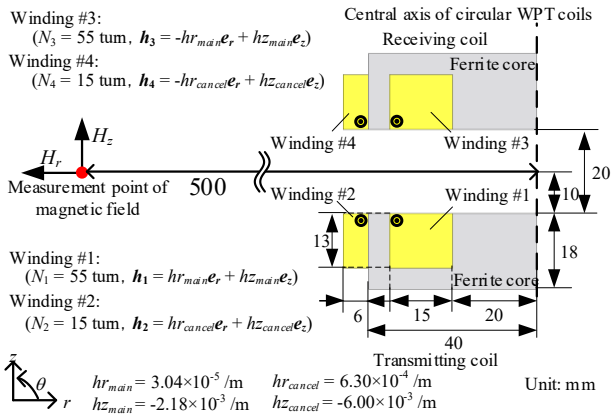


Fig. 4. Measurement point of magnetic field.

The relationship between the current and voltage of the main windings is given by

$$\begin{bmatrix} \dot{V}_1 \\ \dot{V}_3 \end{bmatrix} = j\omega \begin{bmatrix} L_{eqp} & M_{eq} \\ M_{eq} & L_{eqs} \end{bmatrix} \begin{bmatrix} \dot{I}_1 \\ \dot{I}_3 \end{bmatrix} \quad (4)$$

The equivalent self-inductance L_{eqp} and L_{eqs} and the equivalent mutual inductance M_{eq} at the view point of the main windings in Fig. 3(b) are formulated in

$$L_{eqp} = L \left\{ 1 - \frac{(1+\alpha_4)k_c^2 + (1+\alpha_2)k_{ad}^2 - 2k_c k_{sub} k_{ad}}{(1+\alpha_2)(1+\alpha_4) - k_{sub}^2} \right\} \quad (5)$$

$$L_{eqs} = L \left\{ 1 - \frac{(1+\alpha_2)k_c^2 + (1+\alpha_4)k_{ad}^2 - 2k_c k_{sub} k_{ad}}{(1+\alpha_2)(1+\alpha_4) - k_{sub}^2} \right\} \quad (6)$$

$$M_{eq} = L \left\{ k_M - \frac{(2+\alpha_2+\alpha_4)k_c k_{ad} - k_{sub}(k_c^2 + k_{ad}^2)}{(1+\alpha_2)(1+\alpha_4) - k_{sub}^2} \right\} \quad (7)$$

The equivalent inductances L_{eqp} , L_{eqs} and M_{eq} are changed by the operation of the additional power supplies. The variation of L_{eqp} , L_{eqs} and M_{eq} brings errors of the designed transmitting power and resonant frequency of the WPT system. Thus, the parameter variations should be considered in the process of the design or analysis.

B. Leakage Magnetic field

Figure 4 shows the sectional view of the WPT coils and the measurement point of the magnetic field. The measurement point is at the 50-cm horizontal distance from the center of the gap as the representative example. The magnetic field \mathbf{H} at the measurement point is shown in (8) from Biot-Savart law.

$$\begin{aligned} \dot{\mathbf{H}}_{(r,\theta,z)} &= \sum_{m=1}^4 \dot{\mathbf{H}}_{m(r,\theta,z)} = \sum_{m=1}^4 N_m \dot{I}_m \mathbf{h}_m \\ &= \frac{1}{\det L} \left(\dot{V}_p \sum_{m=1}^4 l_{1m} N_m \mathbf{h}_m + \dot{V}_s \sum_{m=1}^4 l_{3m} N_m \mathbf{h}_m \right) \end{aligned} \quad (8)$$

Here, $\det L$ is the determinant of \mathbf{L} , l_{nm} ($n = 1, 2, 3, 4$) is the cofactor of the component (m, n) of \mathbf{L} , $\dot{\mathbf{H}}_{m(r,\theta,z)}$ is the magnetic field generated by \dot{I}_m , \mathbf{h}_m is the vector expressing relationship between $\dot{\mathbf{H}}_{m(r,\theta,z)}$ and \dot{I}_m , and N_m is the turn of winding # m . The vector \mathbf{h}_m is determined by the construction of the WPT coils and the relative distance from the WPT coils to the measurement point. Note that values of \mathbf{h}_m at the measurement point are calculated with electromagnetic field simulation (JSOL, JMAG-Designer).

Equation (8) shows that $\dot{\mathbf{H}}$ is determined by the voltage of

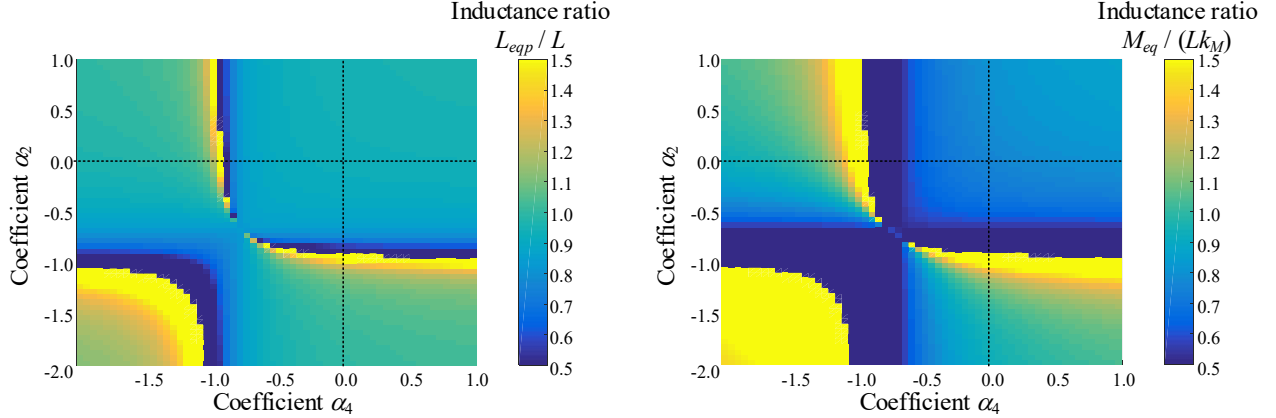


Fig. 5. Parameter variation of equivalent self-inductance and mutual inductance.

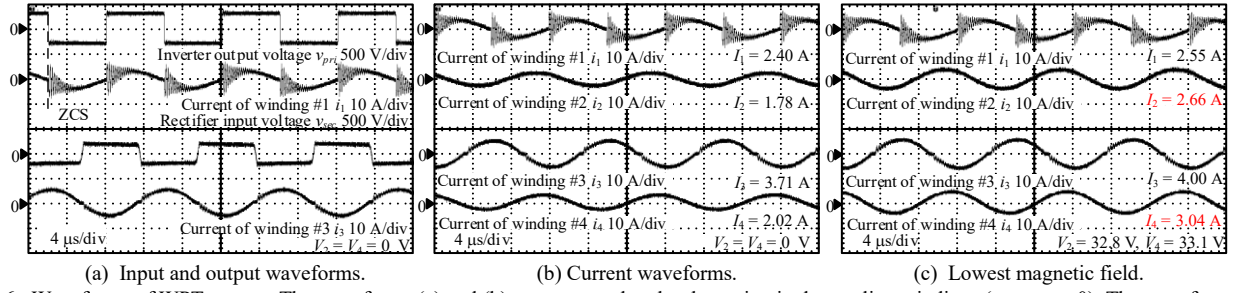


Fig. 6. Waveforms of WPT system. The waveforms (a) and (b) are measured at the short-circuited canceling windings ($\alpha_2 = \alpha_4 = 0$). The waveforms (c) are measured at $1.50 K_{amp}$.

the main windings, the construction of the WPT coils, α_2 and α_4 . The coefficients α_2 and α_4 should be adjusted to achieve minimum H because V_p and V_s are not zero during the power transmission. When the z -axis component H_z of $\mathbf{H}(r, \theta, z)$ is zero, the coefficients α_2 and α_4 are given by

$$\alpha_2 = \alpha_4 = (k_c + k_{ad}) \sqrt{\frac{\mathcal{P}_{main}}{\mathcal{P}_{cancel}}} \frac{hz_{cancel}}{hz_{main}} - (k_{sub} + 1) \quad (9).$$

III. ANALYSIS AND EXPERIMENTAL RESULTS

A. Equivalent Inductance

Figure 5 shows maps of L_{eqp} and M_{eq} with the proposed method. The vertical and horizontal axes are α_2 and α_4 , respectively. The equivalent inductances L_{eqp} and M_{eq} are normalized by L or Lk_M . The coefficients α_2 and α_4 are decreased when the current RMS of the canceling windings is increased with the active shielding. The equivalent inductances L_{eqp} , L_{eqs} and M_{eq} are decreased with the proposed method.

B. Operational Waveforms and Transmitting Power

Figure 6 shows the 600-W operation waveforms. It is noted that the additional power supplies adjust the current RMS of the

canceling windings for simplification. The ratio K_{amp} of the current RMS is defined as

$$K_{amp} = \frac{I_2}{I_{2s}} = \frac{I_4}{I_{4s}} \quad (10),$$

where, I_{2s} and I_{4s} are the current RMS of windings #2 and #4 at the short-circuited canceling windings, respectively.

The circuit is operated under the resonant condition because the phases of the inverter output voltage and the current of the winding #1 are matched. In addition, not only I_2 and I_4 but also I_1 and I_3 are in phase, respectively, at $1.50 K_{amp}$ because of the variation of M_{eq} .

Figure 7 shows the relationship between K_{amp} , α_2 and α_4 . The coefficients α_2 and α_4 become smaller as K_{amp} becomes larger.

Figure 8 shows the output power P_{out} when K_{amp} is changed from 0.5 to 1.5. The output power becomes larger as K_{amp} becomes larger because the transmitting power of the S/S compensated WPT system is inverse proportion to M_{eq} . Thus, the variation of the equivalent inductance with the proposed method is demonstrated.

C. Measured and calculated Leakage Magnetic Field

Figure 9 shows the measured and calculated magnetic field H_z . The magnetic field H_z is calculated under two conditions which are the proposed method and disregarding the variation of I_1 and I_3 . The measured magnetic field is more decreasing by

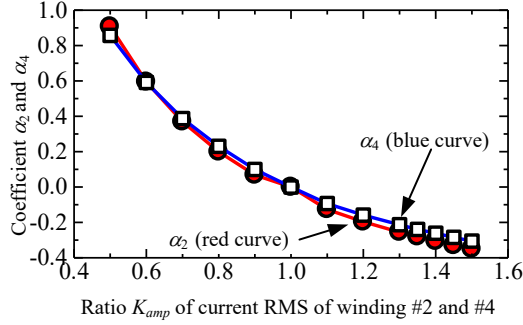


Fig. 7. Variation of α_2 and α_4 with proposed method.

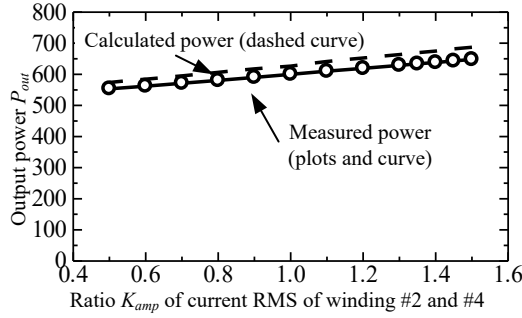


Fig. 8. Measured and calculated output power.

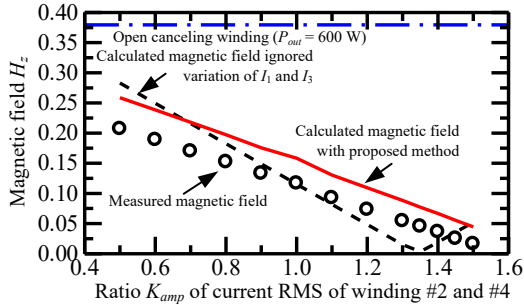


Fig. 9. Magnetic field at measurement point.

27.2dB than H_z of the open canceling windings. Calculated H_z does not match to the measured H_z expecting 1.0 K_{amp} when the variation of I_1 and I_3 is disregarded. Whereas, the trend of H_z with the proposed method agrees with the trend of measured H_z . The error of H_z with the proposed method is probably caused by the parameter mismatch of the WPT coils and calculated error of α_2 or α_4 .

IV. CONCLUSIONS

This paper proposed and analyzed an active-shielding method to reduce EMF of WPT systems. The advantage of the proposed method is that the small-capacity power supplies are available. The magnetic field around the WPT coils is canceled with the additional power supplies and the two canceling. The feature of the proposed method is that the additional power supplies outputs only reactive power such as capacitance. The

parameter variation of the WPT coils and the magnetic field are calculated with the two-port equivalent circuit with the virtual inductance. As a result, the magnetic field decreases by 27.2dB with the proposed method. In addition, the transmitting power is increased as the magnetic field becomes smaller because the equivalent mutual inductance is reduced.

In the future, a current-compensation method will be evaluated when position misalignments of the WPT coils occur.

REFERENCES

- [1] D. Patil, M. K. McDonough, J. M. Miller, B. Fahimi and P. T. Balsara, "Wireless Power Transfer for Vehicular Applications: Overview and Challenges", IEEE Transactions on Transportation Electrification, Vol. 4, No. 1, pp. 3-37 (2018)
- [2] K. Kusaka and J. Itoh: "Development Trends of Inductive Power Transfer Systems Utilizing Electromagnetic Induction with Focus on Transmission Frequency and Transmission Power", IEEJ Journal of Industry Applications, Vol. 137, No. 5, pp. 328-339 (2017)
- [3] G. Lovison, D. Kobayashi, M. Sato, T. Imura and Y. Hori: "Secondary-side-only Control for High Efficiency and Desired Power with Two Converters in Wireless Power Transfer Systems", IEEJ Journal of Industry Applications, Vol. 6, No. 6, pp. 473-481 (2017)
- [4] H. Matsumoto, T. Zaitu, R. Noborikawa, Y. Shibako and Y. Neba: "Control for Maximizing Efficiency of Three-Phase Wireless Power Transfer Systems At Misalignments", IEEJ Journal of Industry Applications, Vol.9, No.4, pp.401-407 (2020)
- [5] International Commission on Non-Ionizing Radiation Protection (ICNIRP), "ICNIRP GUIDELINES FOR LIMITING EXPOSURE TO TIME-VARYING ELECTRIC AND MAGNETIC FIELDS (1HZ – 100 KHZ)", (2010)
- [6] International Commission on Non-Ionizing Radiation Protection (ICNIRP), "ICNIRP GUIDELINES FOR LIMITING EXPOSURE TO ELECTROMAGNETIC FIELDS (100 kHz to 300 GHz)", (2020)
- [7] Ministry of Internal Affairs and Communications, Japan, "Inquiry of technical requirements for wireless power transfer system for EVs in technical requirements for wireless power transfer system in standards of International Special Committee on Radio Interference (CISPR)", (2015)
- [8] E. Asa, M. Mohammad, O. C. Onar, J. Pries, V. Galigekere and G. -J. Su: "Review of Safety and Exposure Limits of Electromagnetic Fields (EMF) in Wireless Electric Vehicle Charging (WEVC) Applications," 2020 IEEE Transportation Electrification Conference & Expo (ITEC), pp. 17-24 (2020)
- [9] K. Inoue, K. Kusaka and J. Itoh: "Reduction in Radiation Noise Level for Inductive Power Transfer Systems using Spread Spectrum Techniques", IEEE Transactions on Power Electronics, Vol. 33, No. 4, pp. 3076-3085 (2018)
- [10] K. Kusaka, K. Furukawa, and J. Itoh: "Development of Three-Phase Wireless Power Transfer System with Reduced Radiation Noise", IEEJ Journal of Industry Applications, Vol. 8, No. 4, pp. 600-607 (2019)
- [11] I. Lee, N. Kim, I. Cho and I. Hong: "Design of a Patterned Soft Magnetic Structure to Reduce Magnetic Flux Leakage of Magnetic Induction Wireless Power Transfer Systems", IEEE Transactions on Electromagnetic Compatibility, Vol. 59, No. 6, pp. 1856-1863 (2017)
- [12] H. Cui, W. Zhong, H. Li, F. He, M. Chen and D. Xu: "A Study on the Shielding for Wireless Charging Systems of Electric Vehicles", 2018 IEEE Applied Power Electronics Conference and Exposition (APEC), pp. 1336-1343 (2018)
- [13] C. Lu, C. Rong, X. Huang, Z. Hu, X. Tao and S. Wang: "Investigation of Negative and Near-Zero Permeability Metamaterials for Increased Efficiency and Reduced Electromagnetic Field Leakage in a Wireless Power Transfer System", IEEE Transactions on Electromagnetic Compatibility, Vol. 61, No. 5, pp. 1438-1446 (2019)
- [14] M. Lu, and K. D. T. Ngo: "Comparison of Passive Shields for Coils in Inductive Power Transfer", 2017 IEEE Applied Power Electronics Conference and Exposition (APEC), pp. 1419-1424 (2017)

- [15] J. Park, D. Kim, K. Hwang, H. H. Park, S. I. Kwak, J. H. Kwon and S. Ahn: "A Resonant Reactive Shielding for Planar Wireless Power Transfer System in Smartphone Application", IEEE Transactions on Electromagnetic Compatibility, Vol. 59, No. 2, pp. 695-703 (2017)
- [16] S. Y. Choi, B. W. Gu, S. W. Lee, W. Y. Lee, J. Huh, and C. T. Rim: "Generalized Active EMF Cancel Methods for Wireless Electric Vehicles", IEEE Transactions on Power Electronics, Vol. 29, No. 11, pp. 5770-5783 (2014)
- [17] K. Furukawa, K. Kusaka and J. Itoh: "General Analytical Model of Inductance Variation by EMF-canceling Coil for Inductive Power Transfer System", IEEJ Journal of Industry Applications, Vol. 8, No. 4, pp. 660-668 (2019)
- [18] S. Cruciani, T. Campi, F. Maradei and M. Feliziani: "Active Shielding Design for Wireless Power Transfer Systems", IEEE Transactions on Electromagnetic Compatibility, Vol. 61, No. 6, pp. 1953-1960 (2019)
- [19] T. Campi, S. Cruciani, F. Maradei and M. Feliziani, "Magnetic Field Mitigation by Multicoil Active Shielding in Electric Vehicles Equipped With Wireless Power Charging System", in IEEE Transactions on Electromagnetic Compatibility, Vol. 62, No. 4, pp. 1398-1405 (2020)
- [20] K. Furukawa, K. Kusaka and J. Itoh: " Low-EMF Wireless Power Transfer Systems of Four-Winding Coils with Injected Reactance-Compensation Current as Active Shielding", 2021 IEEE Applied Power Electronics Conference and Exposition (APEC), pp. 1618-1625 (2021)